6th European Conference on Computational Mechanics (ECCM 6)
7th European Conference on Computational Fluid Dynamics (ECFD 7)
1115 June 2018, Glasgow, UK

MULTIFIDELIY OPTIMIZATION UNDER UNCERTAINTY FOR A SCRAMJET–INSPIRED PROBLEM

FRIEDRICH M. MENHORN[1], GIANLUCA GERACI[2], MICHAEL S. ELDRED[2] AND YOUSSEF M. MARZOUK[3]

[1] Technical University of Munich, Dept. of Informatics
Boltzmannstr. 3, 89748 Garching, Germany
menhorn@in.tum.de

[2] Sandia National Laboratories, Optimization and UQ Dept.
PO BOX 5800 MS 1318, Albuquerque, NM, USA
ggeraci@sandia.gov and mseldre@sandia.gov

[3] Massachusetts Insitute of Technology, Dept. of Aeronautics and Astronautics
Cambridge, MA, USA
ymarz@mit.edu

Key words: Optimization Under Uncertainty, Robust Optimization, Multilevel Monte Carlo, SNOWPAC, DAKOTA

Abstract. SNOWPAC (Stochastic Nonlinear Optimization With Path-Augmented Constraints) is a method for stochastic nonlinear constrained derivative-free optimization. For such problems, it extends the path-augmented constraints framework introduced by the deterministic optimization method NOWPAC and uses a noise-adapted trust region approach and Gaussian processes for noise reduction. In recent developments, SNOWPAC is available in the DAKOTA framework which offers a highly flexible interface to couple the optimizer with different sampling strategies or surrogate models. In this paper we discuss details of SNOWPAC and demonstrate the coupling with DAKOTA. We showcase the approach by presenting design optimization results of a shape in a 2D supersonic duct. This simulation is supposed to imitate the behavior of the flow in a SCRAMJET simulation but at a much lower computational cost. Additionally different mesh or model fidelities can be tested. Thus, it serves as a convenient test case before moving to costly SCRAMJET computations. Here, we study deterministic results and results obtained by introducing uncertainty on inflow parameters. As sampling strategies we compare classical Monte Carlo sampling with multilevel Monte Carlo approaches for which we developed new error estimators. All approaches show a reasonable optimization of the design over the objective while maintaining or seeking feasibility. Furthermore, we achieve significant reductions in computational cost by using multilevel approaches that combine solutions from different grid resolutions.

1 INTRODUCTION

Supersonic Combustion RAMJETS (SCRAMJET) are expected to provide high thrust and low weight for hypersonic flight speeds in the future. Their design has to be robust under uncertain conditions and fulfill high requirements. Due to the high speed, extreme flow conditions are encountered in SCRAMJETs which makes the design challenging. Mixing and combustion must occur within milliseconds, while the flow is supersonic. Challenges are for example to maximize combustion efficiency, while minimizing pressure losses, thermal loading, and the risk of "unstart" or flame blow-out. Thus, a step in the development of robust SCRAMJET designs is their simulation and design optimization under uncertainty (OUU).

This results in a stochastic optimization problem which extends the classical deterministic problem by random parameters $\theta \in \Theta$. They could for example model limited accuracy in measurement data or may reflect a lack of knowledge about model parameters; or, in the SCRAMJET application, inflow parameters like the inlet air velocity, pressure and temperature.

A general approach to tackle such problems is to reformulate the problem where optimizing measures of robustness or risk are used. The idea is to find solutions which are robust despite underlying uncertainty in the parameters. Such an optimization problem [1, 2] has the following form:

$$\begin{aligned} &\min \mathcal{R}^f(\mathbf{x}, \theta), \\ \text{s.t.} \quad &\mathcal{R}^{c_i}(\mathbf{x}, \theta) \leq 0, i = 1, ..., r, \theta \in \Theta. \end{aligned} \tag{1}$$

using so-called measures of robustness or risk $\mathcal{R}^f$ and $\mathcal{R}^c$– over the objective function $f : \mathbb{R}^D \times \Theta \to \mathbb{R}$ and nonlinear inequality constraints $c_i : \mathbb{R}^D \times \Theta \to \mathbb{R}, i = 1, ..., r$ respectively. For now, we are not considering equality constraints of the form $c_i(\mathbf{x}) = 0$. The formulation itself is called robust since we want it to have a certain measure of robustness against uncertainty in the problem. Two typical measures in the mean $\mathbb{E}[\,\cdot\,]$ and variance $\text{Var}[\,\cdot\,]$ which account for the average or the spread of possible realizations, respectively.

With $\mathcal{R}^f$ and $\mathcal{R}^{c_i}$ representing appropriate robustness measures that reflect our optimization goal, we can use sample estimators to approximate the quantities of interest (QoIs). For example, for the approximation of the expected values we draw N samples $\{\theta_i\}_{i=1}^N$ of the uncertain parameters and approximate

$$\mathcal{R}^f[f(\mathbf{x}, \theta)] \approx R^b := \frac{1}{N} \sum_{i=1}^{N} f(\mathbf{x}, \theta_i),$$

using a classical Monte Carlo approach. For simplicity of exposure we only consider Monte Carlo in the following and we will generalize the approach to multilevel Monte Carlo in Section 2.2.

Similar approximations exist for other robustness measures as well. The resulting highly probable upper bound on the sampling error in the approximation of the robustness measures $\mathcal{R}^b$ is denoted by $\varepsilon_b(x)$, i.e.

$$\left|\mathbb{E}[b(\mathbf{x},\theta)] - \frac{1}{N}\sum_{i=1}^{N} b(\mathbf{x},\theta_i)\right| \leq \varepsilon_b(\mathbf{x}),$$

with high probability. Here, b represents either the objective f or constraint c, a naming convention which we will make use of subsequently. It is important to notice that each sample requires a probably computationally expensive evaluation of black-box code limiting the number N of available samples, resulting in significantly large sampling errors $\varepsilon_b(\mathbf{x})$.

The remainder of this paper is organized as follows: In the upcoming section we introduce SNOWPAC, a derivative-free nonlinear stochastic optimization method, that uses a trust region approach and Gaussian Process surrogates to tackle problems of the kind of (1). Moreover, we describe the integration of SNOWPAC into DAKOTA [3]– an uncertainty quantification and optimization library developed by Sandia National Laboratories, which serves as the main driver of the application. Additionally, we present new multi-level Monte Carlo sample and error estimators that are used to evaluate the measures of robustness and risk. As we will see, those error estimators are necessary for SNOWPAC to decide if the trust region can be decreased. In the final section we describe an SCRAMJET–inspired problem which is supposed to show similar behavior as an expensive SCRAMJET simulation; and show optimization results of the application by using our new approach.

2 METHOD

2.1 (S)NOWPAC

NOWPAC is a derivative-free optimization methods based on a trust region approach. In [4] we propose a new way of handling the constraints based on an inner boundary path to compute feasible trial points. Additionally, since the method is derivative-free, it uses a trust region framework based on fully linear models for the objective function and the constraints.

The extension of NOWPAC to stochastic optimization –SNOWPAC (stochastic NOWPAC) [5]– will be of particular interest in this context. SNOWPAC introduces regularized trust region subproblems to improve the efficiency of the optimization process in the presence of noise in the evaluation of the QoIs $\mathcal{R}^b$. It builds local surrogate models m_k^b around the current design x_k within a neighborhood, the trust region, of size ρ_k. Here, $k = 0$ represents the initial design. Additionally, SNOWPAC uses sampling estimators to evaluate and approximate the risk measures.

This, however, introduces noise ε into the evaluations and the surrogate model. Thus, in order to ensure a good quality of the surrogate, we have to enforce an upper bound on the error term $\varepsilon_{max}^k \rho_k^{-2}$, where ε_{max}^k is the maximum noise estimate at step k. We do this by imposing the lower bound

$$\varepsilon_{max}^k \rho_k^{-2} \leq \lambda_t^{-2}, \quad \text{resp.} \qquad \rho_k \geq \lambda_t \sqrt{\varepsilon_{max}^k} = \max_i \lambda_t \sqrt{\varepsilon_i^k}, \tag{2}$$

on the trust region radii for a $\lambda_t \in]0, \infty[$. However, bounding the size of the trust region from below also limits the accuracy of the local surrogate models m_k^b, imposing a bound on the achievable accuracy.

SNOWPAC overcomes this problem by introducing Gaussian process (GP) models as a second "outer" surrogate [6]. Combining local samples with (more global) Gaussian process evaluations reduces the effective sampling error and therefore increases the accuracy of the optimization results.

By combining those two surrogate models SNOWPAC balances two sources of approximation errors. On the one hand, there is the structural error in the approximation of the local surrogate models which is controlled by the size of the trust region radius. On the other hand, we have the inaccuracy in the GP surrogate itself which is reflected by the standard deviation of the GP. Note that SNOWPAC relates these two sources of errors by coupling the size of the trust region radii to the size of the credible interval, only allowing the trust region radius to decrease if the GP posterior estimator becomes small.

SNOWPAC showed promising results in benchmark problems as described in [5], outperforming optimization methods like COBYLA [7], NOMAD [8] or cBO [9]. With its derivative-free approach it offers the flexibility and applicability to a wide range of problems. Thus, it is our method of choice for the SCRAMJET inspired black-box problem. For more details we refer the interested reader to [5].

Moreover, we have successfully integrated SNOWPAC into DAKOTA [3], enabling its use as either a stand-alone optimizer or an approximate subproblem solver (in our case within a MC or MLMC framework). The SNOWPAC package is included as a third party library within the DAKOTA build process, managed by an interface class. This class maps black-box function evaluations for either the deterministic NOWPAC or stochastic SNOWPAC optimizers into evaluations by DAKOTA's general model class, resulting in either a single deterministic simulation or a nested uncertainty analysis, respectively. Mappings for solver specifications, transformations of input variables, standardization of constraint specifications, and reporting of final results are all performed in this wrapper class. A number of unconstrained and constrained verification tests have been performed and benchmark NOWPAC solutions have been added to the DAKOTA nightly test suite.

2.2 MULTILEVEL ERROR ESTIMATORS

In this section we briefly present the MLMC sampling approach that we employed for the UQ to evaluate the mentioned risk measures mean $\mathbb{E}[\,\cdot\,]$ and variance $\mathrm{Var}[\,\cdot\,]$. For an example of application of this method to the a more realistic SCRAMJET problem in the context of forward UQ see [10]. The MLMC method is an efficient sampling strategy that is able to produce more reliable, *i.e.* less variable statistical estimators by resorting to evaluation at many different levels (time resolution and/or spatial discretization for example). For more details please refer to [11]. For a generic QoI Q at a given highest resolution level L ($\ell = 0$ being the coarsest level), a MLMC estimator is computed as

$$\hat{Q}_L = \sum_{\ell=0}^{L} \frac{1}{N_\ell} \sum_{i=1}^{N_\ell} \left(Q_\ell^{(i)} - Q_{\ell-1}^{(i)} \right) = \sum_{\ell=0}^{L} \hat{Y}_\ell, \tag{3}$$

and its variance is given by

$$\mathrm{Var}[\hat{Q}_L] = \sum_{\ell=0}^{L} \frac{1}{N_\ell} \mathrm{Var}[\hat{Y}_L]. \tag{4}$$

Therefore for a sequence of levels for which $Y_\ell \to 0$ with $\ell \to L$, it is possible to redistribute the computational load toward the coarser level in order to reach a desired accuracy. Moreover, the optimal allocation of samples N_ℓ across levels can be obtained in closed form once the variance on each level $\mathrm{Var}[\hat{Y}_L]$ is estimated.

In order to couple a given UQ strategy with SNOWPAC, for a generic objective function $Q \pm \alpha\sigma$ it is necessary to provide an estimation of the standard error SE for both Q and σ. We therefore developed and implemented in the DAKOTA framework (from version 6.7 [3]) the following additional features for the MLMC:

- Derivation of the variance and its standard error for the sample multilevel variance $\mathrm{Var}[Q_L]$, which we denote by s^2_{ML};
- Derivation of the standard error for the sample standard deviation $\sqrt{s^2_L}$ by using the so-called Delta Method.

In addition to the previous points, the former also required the derivation of unbiased (multilevel) estimators up to the fourth order.

The standard error for the sample mean $\hat{Q}_L$ and multilevel sample variance s^2_{ML} are simply obtained as $\sqrt{\mathrm{Var}[\hat{Q}_L]}$, and $\sqrt{\mathrm{Var}[s^2_{ML}]}$, respectively; therefore, no further development are needed for it. However in the following part of the section we highlight the key element that enable us to obtain the SE for the sample standard deviation.

2.2.1 Standard error of the sample variance

The variance of Q_L can be expressed in a multilevel fashion as

$$\mathrm{Var}(Q) = \sum_{\ell=0}^{L} \mathbb{E}\left[(Q_\ell - \mathbb{E}[Q_\ell])^2 - (Q_{\ell-1} - \mathbb{E}[Q_{\ell-1}])^2 \right] = \sum_{\ell=0}^{L} \mathbb{E}[P_\ell^2] - \mathbb{E}[P_{\ell-1}^2] \tag{5}$$

and a sample estimator can be derived for it as

$$s^2_{ML} = \sum_{\ell=0}^{L} (\widehat{P_\ell^2} - \widehat{P_{\ell-1}^2}), \quad \text{where} \quad \hat{P}_\ell^2 = \frac{1}{N_\ell - 1} \sum_{i=1}^{N_\ell} \left(Q_\ell^{(i)} - \hat{Q}_\ell \right)^2. \tag{6}$$

Note that this estimator is unbiased since it is a sum of unbiased estimators once the Bessel correction is adopted to compute each sample variance term $\widehat{P_\ell^2}$. For the variance of s^2_{ML}, given an independent estimator at each level, it follows

$$\mathrm{Var}[s^2_{ML}] = \sum_{\ell=0}^{L} \mathrm{Var}(\widehat{P_\ell^2}) + \mathrm{Var}(\widehat{P_{\ell-1}^2}) - 2\mathrm{Cov}(\widehat{P_\ell^2}, \widehat{P_{\ell-1}^2}), \tag{7}$$

where

$$\mathrm{Var}(\widehat{P_\ell^2}) = \frac{1}{N_\ell}\left(\mu_{4,\ell} - \mathrm{Var}^2(Q_\ell)\right) + \frac{2}{N_\ell(N_\ell - 1)}\mathrm{Var}^2(Q_\ell). \tag{8}$$

In the previous expression, the fourth central moment $\mu_{4,\ell} = \mathbb{E}\left[(Q_\ell - \mathbb{E}\left[Q_\ell\right])^4\right]$ is required therefore its unbiased multilevel estimator has also been derived and implemented in DAKOTA.

In more details the fourth central moment can be written in a multilevel fashion as

$$\mu_L^4 = \mathbb{E}\big[(Q_L - \mathbb{E}[Q_L])^4\big] = \sum_{\ell=0}^{L} \mathbb{E}\big[P_\ell^4 - P_{\ell-1}^4\big] \tag{9}$$

and estimated by

$$s_{ML}^4 = \sum_{\ell=0}^{L} \widehat{P_\ell^4} - \widehat{P_{\ell-1}^4}. \tag{10}$$

Therefore, in order to obtain an unbiased estimator s_{ML}^4 we need unbiased sample estimator for $\widehat{P_\ell^4}$ and $\widehat{P_{\ell-1}^4}$. By means of some lengthy and rather tedious computations it is possible to show that an unbiased estimator $\widehat{P_{\ell-1}^{4,unbiased}}$ can be obtained as a correction of the fourth order sample estimator

$$\widehat{P_\ell^4} = \frac{1}{N_\ell}\sum_{i=1}^{N_\ell}\left(Q_\ell^{(i)} - \sum_{j=1}^{N_\ell} Q_\ell^{(j)}\right)^4, \quad \text{as} \tag{11}$$

$$\widehat{P_\ell^{4,unbiased}} = \frac{1}{N_\ell^2 - 3N_\ell + 3}\left[\frac{N_\ell}{N_\ell - 1}\widehat{P_\ell^4} - (6N - 9)\left(s^2\right)^2\right]. \tag{12}$$

So it will suffice to compute the multilevel fourth order estimator it follows:

$$s_{ML}^{4,unbiased} = \sum_{\ell=0}^{L} \widehat{P_\ell^{4,unbiased}} - \widehat{P_{\ell-1}^{4,unbiased}}. \tag{13}$$

The covariance term that appears in $\mathrm{Var}[s_{ML}^2]$ (see Eq. (7)) is fairly more involved and it can be expressed as

$$\begin{aligned}\mathrm{Cov}(\widehat{P_\ell^2}, \widehat{P_{\ell-1}^2}) = &\frac{1}{N_\ell}\left(\mathbb{E}\left[P_\ell^2 P_{\ell-1}^2\right] - \mathrm{Var}(Q_\ell)\mathrm{Var}(Q_{\ell-1})\right) \\ &+ \frac{1}{N_\ell(N_\ell - 1)}\left(\mathbb{E}\left[Q_\ell Q_{\ell-1}\right] - \mathbb{E}\left[Q_\ell\right]\mathbb{E}\left[Q_{\ell-1}\right]\right)^2,\end{aligned} \tag{14}$$

where

$$\begin{aligned}\mathbb{E}\left[P_\ell^2 P_{\ell-1}^2\right] = &\,\mathbb{E}\left[Q_\ell^2 Q_{\ell-1}^2\right] - 2\mathbb{E}\left[Q_{\ell-1}\right]\mathbb{E}\left[Q_\ell^2 Q_{\ell-1}\right] \\ &+ \mathbb{E}^2\left[Q_{\ell-1}\right]\mathbb{E}\left[Q_\ell^2\right] - 2\mathbb{E}\left[Q_\ell\right]\mathbb{E}\left[Q_\ell Q_{\ell-1}^2\right] \\ &+ 4\mathbb{E}\left[Q_\ell\right]\mathbb{E}\left[Q_{\ell-1}\right]\mathbb{E}\left[Q_\ell Q_{\ell-1}\right] + \mathbb{E}^2\left[Q_\ell\right]\mathbb{E}\left[Q_{\ell-1}^2\right] - 3\mathbb{E}^2\left[Q_\ell\right]\mathbb{E}^2\left[Q_{\ell-1}\right].\end{aligned} \tag{15}$$

Note the computation of an unbiased estimator for the latter covariance term is not difficult to derive once unbiased estimators for the mean and variance are available.

2.2.2 Standard Error for the sample standard deviation

Unfortunately the SE for the multilevel standard deviation cannot be derived in closed form exactly. This is also the case for a single level sample standard deviation s. It is usually possible to resort to two approximations. The first is to assume that the distribution of the population is normal. In this case an exact expression for the standard error $SE(s)$ can be derived as

$$SE(s) = \frac{\sqrt{s^2}}{2(N-1)}. \tag{16}$$

However, in practice the distributions of the QoIs are not normal and, therefore the previous expression is only an approximation. The second approximation is to apply the so-called Delta Method which enable us to approximate the probability distribution of a function (the root mean square for us) of an asymptotically normal estimator, *i.e.* the sample variance in our case. Of course, in our case the sample variance is not an asymptotically normal estimator, therefore this is only an approximation. Therefore, for a generic estimator θ, the SE of its generic function $f(\theta)$ is given by

$$SE(f(\theta)) \approx |g'(\theta)| SE(\theta). \tag{17}$$

For us, $\theta = s^2_{ML}$ and $f(\theta) = \theta^{1/2}$, so it follows that

$$SE(\sqrt{s^2_{ML}}) \approx \frac{1}{2\sqrt{s^2_{ML}}} \sqrt{\mathrm{Var}[s^2_{ML}]}. \tag{18}$$

3 NUMERICAL RESULTS

In order to accelerate the testing and refinement of the algorithms, we designed a model problem that is related to the SCRAMJET problem but which executes much more rapidly. This allows us to perform an entire OUU workflow in a few hours. In direct support of the OUU algorithmic development, this offers capabilities to more thoroughly compare the performance of different OUU strategies.

The test problem consists of a 2D inviscid flow through a duct with geometry inspired by the 2D SCRAMJET problem. We designed three resolution levels, namely COARSE, MEDIUM and FINE, that can provide a multilevel capability and run in about 10s, 30s and 300s respectively. The software selected for this test case is the Stanford University Unstructured Code (SU2) [12] while for the meshing capability we used gmsh [13]. In particular, for each design (which involves a unique domain geometry) the geometry is obtained from gmsh and the CFD is performed with SU2 once the inlet conditions are fully specified. The mesh discretizations are reported in Figure 1 where both COARSE, MEDIUM and FINE resolutions are shown for reference.

The test problem is designed to mimic the shock wave pattern of the SCRAMJET problem. This task is accomplished by introducing a wedge in a location where the primary injector is eventually located. The role of the wedge is to deflect the flow in order to generate a shock wave that can reflect against the walls and interact with the rarefaction waves obtained in the region of the cavity where the section of the duct abruptly increases.

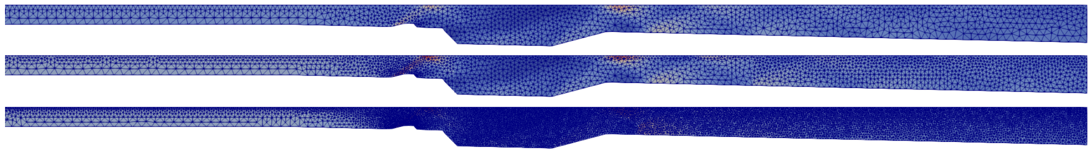

Figure 1: Different mesh sizes used for the multilevel approach. From top to bottom: COARSE, MEDIUM and FINE.

The geometry of the bump is parameterized in order to provide five design parameters for the OUU (same dimensionality as the SCRAMJET). A cartoon of the wedge with the definition of the five design parameters is reported in Figure 2. The bounds for the design parameters, $\mathbf{x}$, and uniform parameters, ξ, are given in the following Table 1 with their respective lower and upper bounds:

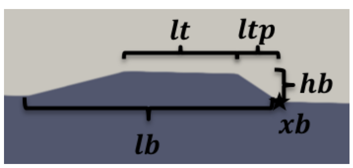

Figure 2: Design parameters for the SU2 supersonic duct problem.

Design parameters $\mathbf{x}$	Uncertain parameters ξ
$0.5 \leq hb \leq 2.5$	$p_{0,in} \sim \mathcal{U}(1.332e6, 1.628e6)$
$7.5 \leq lt \leq 11.5$	$T_{0,in} \sim \mathcal{U}(1.395e3, 1.705e3)$
$2.5 \leq ltp \leq 4.5$	$M_{in} \sim \mathcal{U}(2.259e0, 2.761e0)$
$17.5 \leq lb \leq 20.5$	
$79.5 \leq xb \leq 85.5$	

Table 1: Design and uncertain parameters and their respective lower and upper bounds.

The inlet conditions for the problem are fully determined by the stagnation pressure $p_{0,in}$, temperature $T_{0,in}$ and the Mach number M_{in}. We consider these three parameters to be uncertain, while their nominal values are consistent with the SCRAMJET inlet condition.

The OUU problem to be solved is the following:

$$\begin{aligned} P^*_{\text{loss}}(\mathbf{x}^*) &= \min_{\mathbf{x}} \mathbb{E}[P_{\text{loss}}(\mathbf{x}, \theta)] \\ \text{s.t. } & 440 \leq \mathbb{E}[T_{\text{c}}(\mathbf{x}, \theta)] - 3\sigma[T_{\text{c}}(\mathbf{x}, \theta)], \end{aligned}$$

where the objective function P_{loss} and the constraint T_{c} are defined as follows:

$$\begin{aligned} P_{loss} &= \left(P_0^{in} - \frac{1}{L_y} \int_{\text{out}} P_0(y) \mathrm{d}y \right) / P_0^{in} \\ T_{\text{c}} &= \frac{1}{L_x} \int_{L_c} T(x) \mathrm{d}x, \end{aligned}$$

where L_c describes the length of the cavity domain, used for computing the average cavity temperature.

We consider in the following three separate strategies to be embedded in the OUU workflow with DAKOTA+(S)NOWPAC with the given nomenclature used in the upcoming sections:

- (DET) DAKOTA+NOWPAC deterministic optimization at nominal value of stochastic parameters

- (MC) DAKOTA+SNOWPAC using Monte Carlo sampling estimators with 54 samples on the FINE grid
- (MLMC) DAKOTA+SNOWPAC using multilevel Monte Carlo sampling estimators with 179 samples on the COARSE grid, 20 samples on the MEDIUM-COARSE and 5 samples on the MEDIUM-FINE discrepancy. This profile was selected by matching the accuracy of the MC estimator with 54 samples on the FINE grid.

In Table 2 we compare the different results obtained from the three methods of choice. Overall, we receive slightly different designs for the three strategies, and MC shows the best objective value. Moreover, the lower constraint is active for the stochastic methods. Regarding the cost, we can see the advantage of using MLMC compared to MC: we reduce the number of FINE grid evaluations from 4320 for MC to 400 for MLMC.

Problem	$\mathbf{x}^*$	$\mathbf{p}^*_{\text{loss}}$	$\mathbf{c}^*$	**Cost** (C, M, F)
DET	$[1.86, 11.32, 2.5, 17.71, 79.55]$	0.4931	602.3990	(0, 0, 80)
MC	$[2.10, 9.65, 4.5, 20.5, 79.5]$	0.4780	447.7121	(0, 0, 4320)
MLMC	$[2.24, 7.50, 2.50, 17.50, 79.50]$	0.4906	442.3871	(15920, 2000, 400)

Table 2: The table shows the design $\mathbf{x}^*$, objective $\mathbf{p}^*_{\text{loss}}$, constraint $\mathbf{c}^*$ and cost for the different methods on different resolutions COARSE (C), MEDIUM (M) and FINE (F) after 80 evaluations steps when DET has converged.

As can be seen in the table and also already suggested in benchmark results in [4], NOWPAC converges and find a local optima quickly after 80 steps since there is no noise restriction on the trust region. The constraint is not getting active in this case.

By introducing uncertainty into the problem we can see its influence in the noisy evaluations. The evolution of the objective (left) and constraint (right) for the two stochastic approaches are reported in Figures 3 and 4. While the dashed, lighter colored lines show the evaluations of the optimizer in the current step, the dark blue and dark green color show the optimal value and respective constraint. In the constraint plots, we further depict the mean value of the constraint. In both cases the optimizer finds a lower optima compared to the deterministic optimization while the constraint is active for most of the optimization progress. Moreover, we see the effect of the introduced push back on the constraint such that the mean constraint value of the design is kept back in the feasible domain.

Finally, regarding the MLMC approach we see a similar initial behavior of the optimization progress compared to MC, although the final objective found is higher and the optimizer gets stuck in a corner of the optimization domain; all design box constraints are active. Additionally, the nonlinear constraint is active as well. Despite the savings in computational cost, however, we can see progress in the optimization.

The flow field of the pressure of the final designs compared to the starting design is shown in Figure 5 from top to bottom: starting design, DET, MC and MLMC. Although

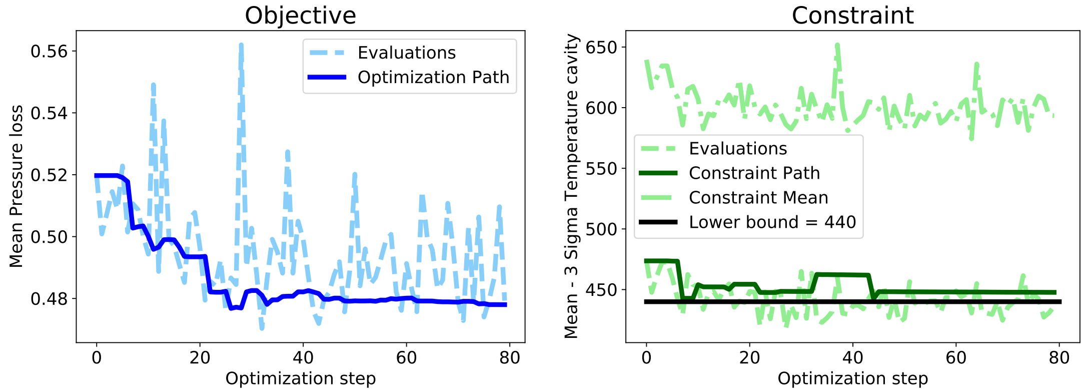

Figure 3: Objective and constraint evolutions for the OUU problem using MC.

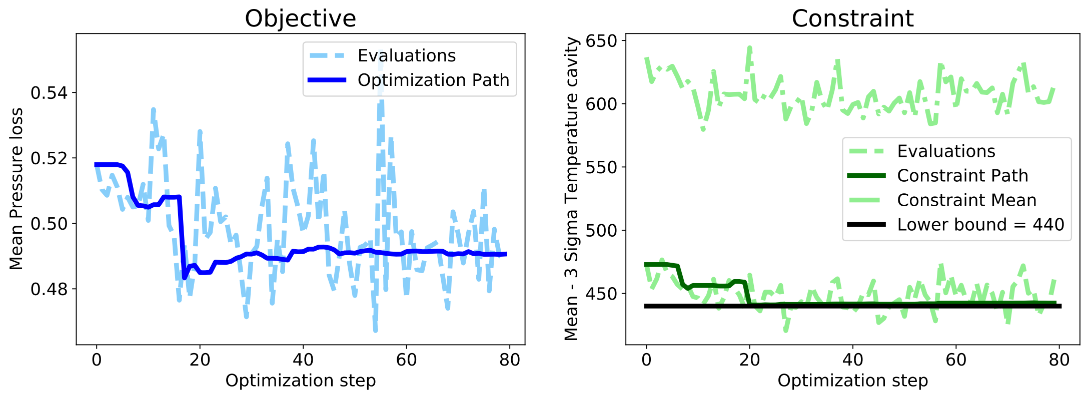

Figure 4: Objective and constraint evolutions for the OUU problem using MLMC.

we reach different designs we see the attenuating effect on the initial shockwave induced by the decreased slope or height of the wedge. Relating these illustrative with the qualitative results from the table we deduce further that the objective functions inhibits multiple local minima found by the different optimization approaches.

Due to high noise in the estimators we only see a slow convergence in the stochastic methods MC and MLMC. Because of that the trust regions size shrinks slowly and we selected a maximum number of optimization steps as stopping criteria. Regarding the optimization plot as well, there is not much progress visible after about 50 iterations steps for MC as well as MLMC.

4 CONCLUSION

We presented current results for optimization under uncertainty for a SCRAMJET inspired problem by using the derivative-free optimization method SNOWPAC and newly developed error estimators for multilevel sampling. Those error estimators are necessary

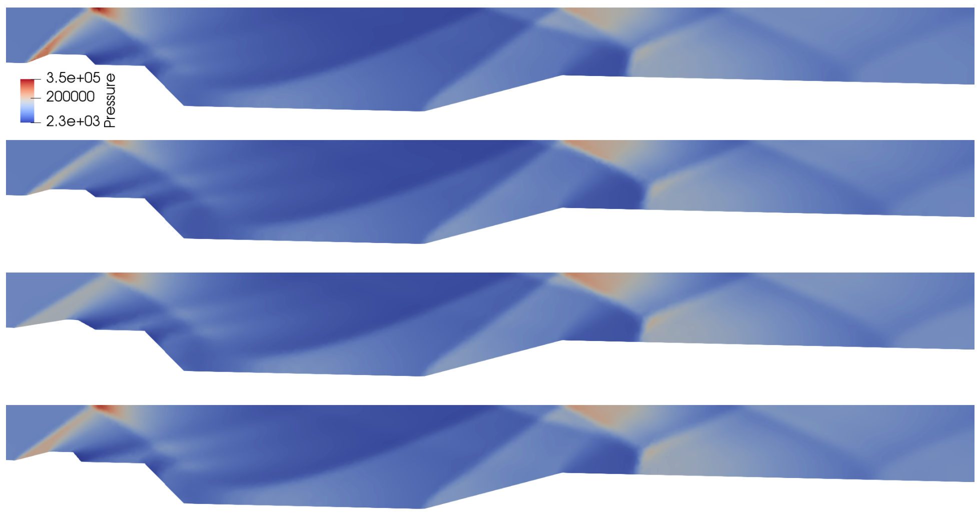

Figure 5: Different final designs obtained after optimization using the presented methods compared to the starting design. From top to bottom: starting design, DET, MC and MLMC.

since SNOWPAC requires noise estimates for its trust region management and progression in the optimization. The obtained results show optimization progress for the deterministic case, classic Monte Carlo estimators as well as the new multilevel approach. However, in the two robust optimization scenarios we can see the performance advantage of using a multilevel approach by significantly reducing the number of evaluations on the highest resolution grid thereby reducing the overall computational cost considerably. Those results were all computed by using the framework offered by DAKOTA which now supplies (S)NOWPAC as a optimization methods. In further studies we will investigate the behavior for different risk measures like chance constraints or conditional value at risk. Additionally, using the possibilities of DAKOTA we will consider different approaches to estimate the measures of robustness and risk and also exploit the performance advantage due to, e.g. its intrinsic possibilities for parallelism.

5 ACKNOWLEDGEMENTS

Support for this research was provided by the DARPA program EQUiPS. Sandia National Laboratories is a multimission laboratory managed and operated by National Technology & Engineering Solutions of Sandia, LLC, a wholly owned subsidiary of Honeywell International Inc., for the U.S. Department of Energy's National Nuclear Security Administration under contract DE-NA0003525. The views expressed in the article do not necessarily represent the views of the U.S. DOE or the United States Government.

REFERENCES

[1] A. Ben-Tal and A. Nemirovski. Robust solutions of uncertain linear programs. *Oper. Res. Lett.*, August 1999, **25**(1):1–13.

[2] H.-G. Beyer and B. Sendhoff. Robust optimization–a comprehensive survey. *Computer Methods in Applied Mechanics and Engineering*, 2007, **196**(33):3190–3218.

[3] B. Adams, L. Bauman, W. Bohnhoff, et al. Dakota, a multilevel parallel object-oriented framework for design optimization, parameter estimation, uncertainty quantification, and sensitivity analysis - version 6.6 users manual, July 2014. Updated May, 2017.

[4] F. Augustin and Y. M. Marzouk. A path-augmented constraint handling approach for nonlinear derivative-free optimization. *arXiv:1403.1931v3*, 2014.

[5] F. Augustin and Y. M. Marzouk. A trust-region method for derivative-free nonlinear constrained stochastic optimization. *arXiv:1703.04156*, 2017.

[6] C. E. Rasmussen and C. K. I. Williams. *Gaussian Processes for Machine Learning.* MIT Press, 2006.

[7] M. J. D. Powell. A View of Algorithms for Optimization Without Derivatives. *Mathematics TODAY*, 2007, **43**(5).

[8] S. Le Digabel. NOMAD: Nonlinear optimization with the MADS algorithm. *ACM Trans. Math. Softw.*, 2011, **37**:44.

[9] J. R. Gardner, M. J. Kusner, Z. Xu, K. Q. Weinberger, and J. P. Cunningham. Bayesian optimization with inequality constraints. In *Proceedings of the 31st International Conference on International Conference on Machine Learning - Volume 32*, ICML'14, pages II–937–II–945. JMLR.org, 2014.

[10] G. Geraci, M. S. Eldred, and G. Iaccarino. A multifidelity multilevel Monte Carlo method for uncertainty propagation in aerospace applications. In *19th AIAA Non-Deterministic Approaches Conference*, AIAA SciTech Forum. American Institute of Aeronautics and Astronautics, January 2017.

[11] M. B. Giles. Multilevel Monte Carlo Path Simulation. *Operations Research*, June 2008, **56**(3):607–617.

[12] T. D. Economon, F. Palacios, S. R. Copeland, T. W. Lukaczyk, and J. J. Alonso. SU2: An Open-Source Suite for Multiphysics Simulation and Design. *AIAA Journal*, dec 2015, **54**(3):828–846.

[13] C. Geuzaine and J. Remacle. Gmsh: A 3-D finite element mesh generator with built-in pre- and post-processing facilities. *International Journal for Numerical Methods in Engineering*, 2009, **79**(11):1309–1331.